

Article pubs.acs.org/cm

# Improving the Purity and Uniformity of Pd and Pt Nanocrystals by Decoupling Growth from Nucleation in a Flow Reactor

Ruhui Chen, Zhiheng Lyu, Yifeng Shi, and Younan Xia\*



Cite This: Chem. Mater. 2021, 33, 3791-3801



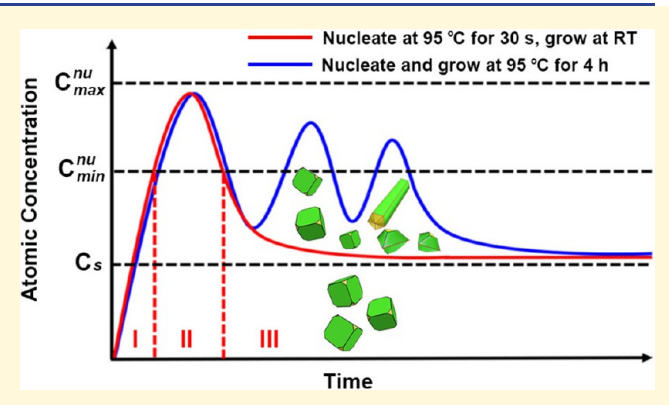
**ACCESS** I

Metrics & More

Article Recommendations

Supporting Information

ABSTRACT: Despite significant progress in controlling the synthesis of noble-metal nanocrystals, the purity and uniformity of many products are still plagued by the unwanted nucleation events taking place in the growth stage. To this end, it is necessary to decouple growth from nucleation during a colloidal synthesis of nanocrystals. Taking Pd nanocubes as a typical example, here, we demonstrate that nucleation and growth can be separated from each other by re-designing the experimental setup while manipulating the reduction pathway of the precursor. Specifically, we pump the reaction solution through a tubular flow reactor and trigger a single burst of nucleation by subjecting the solution to an elevated temperature for a very short period of time to enable solution-phase reduction. The solution is then kept at room temperature for slow growth through surface reduction, producing



pure and uniform Pd nanocubes. Due to the elimination of additional nucleation events during growth, the products exhibit high uniformity in terms of both size and shape. We elucidate the mechanistic details by quantitatively analyzing the reduction kinetics and monitoring the nanocrystals obtained at different stages of the synthesis. We further investigate the impacts of both temperature and duration of nucleation on the diversity of seeds and the quality of the resultant nanocrystals. This methodology has also been extended to the preparation of sub-5 nm Pt nanocubes and is potentially applicable to the synthesis of other types of colloidal nanocrystals.

## ■ INTRODUCTION

Significant progress has been made in tailoring the properties of noble-metal nanocrystals and thus enhancing their performance in various applications by engineering their size, shape, and internal structure. 1-5 The success is built upon our mechanistic understanding of the nucleation and growth steps typically involved in the colloidal synthesis of nanocrystals. Of particular importance, it is generally accepted that homogeneous nucleation and growth have to be decoupled from each other in order to obtain pure and uniform samples.<sup>6–8</sup> A simple explanation can be found in the LaMer model that was formulated more than half a century ago to guide the colloidal synthesis of monodispersed spherical particles made of elemental sulfur.6 According to this model, there should be only one burst of homogeneous nucleation, followed by the growth of the just-formed seeds, in order to achieve monodispersity in particle size. If homogeneous nucleation occurs multiple times throughout a synthesis, in particular, after growth has already started, the products will suffer from size polydispersity. When applied to a colloidal synthesis of metal nanocrystals, the polydispersity may also include other aspects such as shape, morphology, and/or internal structure.

While the LaMer model clearly points out the general requirement for obtaining pure and uniform samples of metal nanocrystals, it is nontrivial to meet such a requirement experimentally. In many cases, homogeneous nucleation can take place multiple times before the concentration of the monomer eventually drops to a level low enough to suppress homogeneous nucleation while allowing for heterogeneous nucleation and growth on the just-formed seeds. In a recent study, we addressed this issue by supplying the precursor in two fractions, with a small fraction (about 5% of the total amount) used for the formation of seeds via homogeneous nucleation while the majority is added at a later point for heterogeneous nucleation and growth.9 The success of this approach critically depends on the selection of a precursor with the right reduction pathway. Recent studies indicated that the precursor involved in a colloidal synthesis of metal nanocrystals could undergo direct reduction to the atomic form in a solution phase or adsorb onto the surface of the just-formed

Received: March 16, 2021 Revised: April 21, 2021 Published: May 3, 2021





seeds, followed by reduction to atoms. 10-14 Ideally, the precursor should take the solution-phase reduction pathway during the stage of homogeneous nucleation, and immediately switch to surface reduction upon entering the growth stage. Such a switching can be potentially achieved through the regulation of reduction kinetics by manipulating experimental parameters such as the reaction temperature. <sup>14</sup> For example, an elevated temperature and thus a fast reduction rate can be imposed at the beginning of a synthesis to enable homogeneous nucleation through solution-phase reduction for the generation of seeds. Afterward, the temperature can be lowered to slow down the reduction kinetics, limiting the reduction to the surface of the just-formed seeds while suppressing additional homogeneous nucleation. In this way, the nucleation and growth of a colloidal synthesis of metal nanocrystals will be naturally separated from each other. For this approach to work, it is vital to keep the reaction system at an elevated temperature for a duration as short as possible. Otherwise, multiple nucleation events may still occur when the solution is held at the elevated temperature.

The conventional batch reactor should be replaced with a tubular flow reactor to achieve the required jump in temperature over a period of time as short as possible. Considering the slowness in terms of heat transport from the surrounding (e.g., the oil bath) to the reaction solution hosted in a typical vial of 23 mm in outer diameter, it is expected to take at least several minutes to attain a uniform temperature for the reaction solution. When switched to a tubular flow reactor of 1.6 mm in outer diameter and 0.8 mm in inner diameter, it should be feasible to equilibrate the temperature of the reaction solution with the surroundings (e.g., an oil bath) within a few seconds, if not sooner. The same argument also applies to the cooling process when the heated reaction solution needs to be quickly brought to a lower temperature for the prevention of additional homogeneous nucleation. As an additional advantage, one can easily manipulate the duration of heating applied to the reaction solution in a flow reactor by controlling the flow rate and/or the length of the segment subjected to heating. In recent years, flow reactors have been increasingly applied to the synthesis of colloidal nanocrystals for their advantages such as the linear scalability, rapid screening of experimental parameters, improved control over mass and heat transfers, and distance to time transformation. 15-19

In prior studies, flow reactors have been explored to separate growth from nucleation for the preparation of inorganic nanoparticles with enhanced properties. In one example, solutions containing Fe(III) and OH-, respectively, were flushed into a coaxial-flow device to trigger nucleation, followed by growth at an elevated temperature for the synthesis of  $\alpha$ -FeOOH nanoparticles.<sup>20</sup> In this case, a gradient in the spatial distribution of the pH value in the stream made it difficult to exclude the involvement of multiple nucleation events in the synthesis, as indicated by the observation of aggregated nuclei after the completion of synthesis. In another two examples, a dual-stage flow reactor was utilized to synthesize colloidal quantum dots of PbS and CuInSe2, respectively, with improved size distributions and optical properties. The precursors were mixed and then flown through two zones held at different temperatures, with the first zone heated to a higher temperature to trigger nucleation, while the second zone maintained at a lower temperature for continuous growth. Although the nucleation and growth stages

were physically isolated, multiple nucleation events might still occur during the nucleation or the "growth-only" stage, as Ostwald ripening was proposed to be involved in the growth process. While these studies nicely demonstrated the ability to obtain colloidal nanocrystals with enhanced properties by separating growth from nucleation, the extension of this approach from semiconductors to metals might still face complications due to the involvement of different reduction kinetics. As a major difference, the synthesis of metal nanocrystals typically involves the reduction of a precursor, which may proceed through solution and surface pathways depending on the reduction rate. Besides, the nucleation and growth processes not only affect the size distribution of metal nanocrystals but also determine their internal structure, shape, and morphology. <sup>7,8</sup> For a dual-stage synthesis of Ag nanocubes that involved nucleation under microwave heating, followed by growth at a lower temperature, the nanocubes could only be obtained at a maximal purity of 78%.<sup>23</sup> In addition to decoupling growth from nucleation, it is necessary to manipulate the reduction pathways of the precursor in order to obtain metal nanocrystals with higher purity and uniformity.

Taking the synthesis of Pd nanocubes as an example, here we demonstrate a methodology for separating growth from nucleation by switching from the conventional batch reactor to a tubular flow reactor and by leveraging the two distinctive reduction pathways of a precursor. Specifically, by flowing the pre-mixed reaction solution through a fluidic tube held at an elevated temperature, solution-phase reduction can be enabled over a well-controlled period of time as short as 10 s to trigger a single burst of nucleation. The just-formed seeds are then allowed to grow at room temperature through surface reduction only, generating Pd nanocrystals with high purity and good uniformity. By quantitatively analyzing the reduction kinetics and monitoring the growth process, we validate that additional nucleation is suppressed to ensure good uniformity and purity for the final products. We also investigate the effects of temperature and duration of nucleation on the quality of the resultant nanocrystals, shedding new light on the mechanistic details of such a synthesis. This method has also been successfully extended to the synthesis of sub-5 nm Pt nanocubes highly uniform in terms of size and shape.

# **■ EXPERIMENTAL SECTION**

Chemicals and Materials. Potassium tetrabromopalladate(II) ( $K_2PdBr_4$ ), potassium bromide (KBr, 99.0%), poly(vinyl pyrrolidone) (PVP,  $M_w \approx 55,000$ ), L-ascorbic acid (AA, 99.0%), sodium hexachloroplatinate(IV) hexahydrate ( $Na_2PtCl_6\cdot 6H_2O$ , 98%), and ethylene glycol (EG, anhydrous, 99.8%) were all obtained from Sigma-Aldrich. All chemicals were used as received. Deionized (DI) water with a resistivity of 18.2 M $\Omega$ ·cm at room temperature was used throughout the experiments.

Separation of Growth from Nucleation Using a Fluidic Device. For a standard protocol, 34.4 mg of  $K_2PdBr_4$ , 240 mg of KBr, 44 mg of PVP, and 21.1 mg of AA were dissolved in 4 mL of water. The mixture was stirred at room temperature for 15 min to obtain the reaction solution. As shown in Figure 1a, the fluidic device consisted of a polytetrafluoroethylene (PTFE) tube with an inner diameter of 0.8 mm, a plastic syringe, and a syringe pump. Prior to the introduction of the reaction solution, a segment of the PTFE tube was immersed in an oil bath held at 95 °C and heated for 20 min. Afterward, the reaction solution was pumped into the tube at a flow rate of 2 mL/min to thermally trigger the reduction of the precursor for the initiation of nucleation in the reaction solution. By varying the length of the segment being heated, the duration of nucleation could be tightly controlled and shortened down to a few seconds. When 204

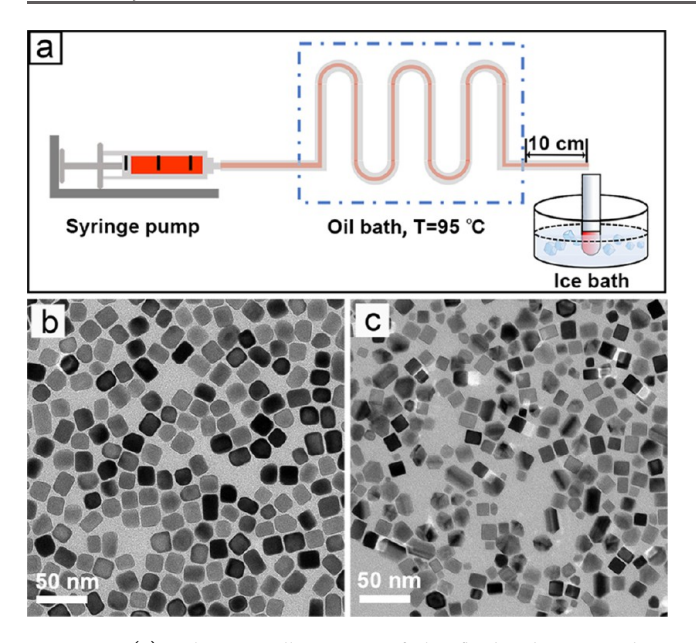


**Figure 1.** (a) Schematic illustration of the fluidic device used to control the nucleation step prior to the formation of nanocrystals. (b) TEM image of slightly truncated Pd nanocubes prepared by conducting the nucleation at 95 °C for 30 s, followed by growth at room temperature for 48 h. (c) TEM image of Pd nanocrystals obtained by conducting the synthesis in a vial at 95 °C for 4 h.

cm of the PTFE tube was immersed in the oil bath, for example, the duration of nucleation would be 30 s only. After passing through the oil bath, the reaction solution containing the just-formed seeds was collected in a tube placed in an ice bath to immediately quench the reduction reaction and thereby eliminate additional nucleation. The length of the tube from the point of leaving the oil bath to the point of entering the ice bath was kept at 10 cm to minimize additional nucleation after the reaction solution had left the oil bath. Finally, the collected solution was kept at room temperature (22 °C) under magnetic stirring, allowing the seeds to grow slowly over a period of 48 h. The final Pd nanocrystals were collected by centrifugation, washed three times with water, and re-dispersed in water for further characterization.

Quantitative Analysis of the Reduction Kinetics. We used ultraviolet—visible (UV—vis) spectroscopy to analyze the reduction kinetics by measuring the concentration of Pd(II) ions remaining in the solution after the reaction had proceeded for different periods of time. Two reaction solutions were prepared in parallel under the same conditions as specified in the standard protocol, with one of the solutions being kept at room temperature without undergoing nucleation in the fluidic device. At various time points, an aliquot of 0.2 mL was sampled from the solution and quickly injected into 0.8 mL of aqueous KBr (500 mg/mL) held at 0 °C to quench the reduction. After centrifugation at 55,000 rpm for 30 min to remove all the Pd nanoparticles, the supernatant was further diluted by 20 times with aqueous KBr (400 mg/mL) prior to UV—vis measurement. By comparing the absorbance at 332 nm with a calibration curve, the concentrations of PdBr<sub>4</sub> $^{2-}$  ions remaining in the reaction solution were derived.

The calibration curve, as shown in Figure S1, is obtained from a set of  $PdBr_4^{2-}$  solutions with different concentrations. A stock solution of 25 mM in concentration was prepared by dissolving 12.6 mg of  $K_2PdBr_4$  in 1 mL of aqueous solution containing 60 mg of KBr, and then diluted to different concentrations for UV—vis measurements. Aqueous KBr solution (400 mg/mL) was used for the dilution to ensure that the Pd(II) ions remained in the form of  $PdBr_4^{2-}$ .

Extension to the Preparation of Sub-5 nm Pt Nanocubes. The synthetic protocol for Pt nanocubes is similar to that for Pd nanocubes, except for the differences in the solvent and reducing

agent. In a typical synthesis, 3 mL of the EG solution containing 50 mg of PVP and 21 mg of KBr were heated at 100 °C for 7 min to fully dissolve the solids and then cooled down to room temperature. At the same time, 10 mg of Na<sub>2</sub>PtCl<sub>6</sub>·6H<sub>2</sub>O was dissolved in 2 mL of EG under sonication. To verify whether there were reduction and nucleation during sonication, the as-obtained precursor solution was centrifuged at 100,000 rpm for 1 h and no solid precipitate was observed. Besides, as confirmed by inductively coupled plasma-mass spectroscopy, the concentration of the Pt(IV) ions remaining in the "supernatant" showed no change before and after sonication. The two EG solutions containing surfactants and Pt(IV) precursors, respectively, were then mixed and stirred at room temperature for 15 min to obtain a homogeneous reaction solution. By flowing the solution in a tubular reactor held at 185 °C, the homogeneous nucleation was initiated for a duration of 60 s. followed by slow growth at 110 °C for 48 h. The resultant Pt nanocubes were collected by centrifugation and washed with water for further characterization.

**Characterization.** The transmission electron microscopy (TEM) images were taken using a Hitachi HT7700 microscope operated at 120 kV. Prior to TEM analysis, a suspension of the nanocrystals was drop casted on the carbon-coated copper grid and allowed to dry under ambient conditions. Quantitative analysis of the reduction kinetics was performed through the use of a UV—vis spectrophotometer (Cary 60, Agilent Technology).

## ■ RESULTS AND DISCUSSION

As illustrated in Figure 1a, the fluidic device we used for triggering the nucleation of Pd nanocrystals is comprised a PTFE tube with one segment immersed in an oil bath. In a standard process, the reaction solution was introduced into the PTFE tube using a syringe pump. When the solution flowed through the oil bath held at 95 °C, a burst of nucleation would be triggered, during which PdBr<sub>4</sub><sup>2-</sup> was quickly reduced by AA in the solution to generate nuclei and then seeds via homogeneous nucleation. In the standard protocol, the duration of nucleation was set to 30 s by adjusting the length of the tube being immersed in the oil bath. The reduction was immediately quenched upon collecting the solution in a tube held in an ice bath. Afterward, the seeds were allowed to grow at room temperature for up to 48 h. Because the nucleation process is extremely sensitive to the spatial distribution of temperature in the solution, the PTFE tube with an inner diameter of 0.8 mm was used to ensure the quick homogenization of the temperature inside it. It is worth noting that the temperature of the reaction solution was still high after leaving the oil bath but before entering the ice bath, and this might lead to additional, undesired nucleation. For this reason, the length of this segment of the tube was kept at a relatively short length of 10 cm. At a flow rate of 2 mL/min, it should take less than 1.5 s for the solution to flow through this segment and enter the ice bath, helping suppress the formation of additional seeds.

It should be emphasized that the precursor to Pd also needs to be judiciously selected in order to control the reduction pathways involved in the nucleation and growth steps of the synthesis. Different from  $PdCl_4^{2-}$ , another precursor commonly used in the preparation of Pd nanocrystals,  $PdBr_4^{2-}$  features a slower reduction kinetics because of its more negative standard reduction potential ( $PdBr_4^{2-}/Pd = 0.49 \text{ V}$ ,  $PdCl_4^{2-}/Pd = 0.62 \text{ V}$  vs reversible hydrogen electrode or RHE). When reduced by AA in aqueous solution,  $PdBr_4^{2-}$  favors the solution reduction pathway at an elevated temperature, while switching to surface reduction at room temperature in the presence of preformed seeds. Note that the amount of KBr used in a standard synthesis was in large

excess, helping preserve the Pd(II) ions in the form of PdBr<sub>4</sub><sup>2-</sup> and regulate the reduction kinetics. 25 Figure 1b shows a typical TEM image of the Pd nanocrystals prepared using the standard protocol. Due to the presence of Br ions as a capping agent toward Pd{100} facets, we obtained slightly truncated nanocubes with an average length of 18.2 ± 1.9 nm and an aspect ratio of 1.2  $\pm$  0.2. The slight truncation at the corners could be possibly ascribed to the extremely slow growth rate, resulting in the kinetically controlled products not fully stabilized by the capping agent, which was also observed in a previous study.<sup>25</sup> Moreover, owing to the localized oxidative etching induced by the Br ions and oxygen in the reaction solution, the capping agent could be selectively removed from one of the side faces of the nanocube, leading to the preferential deposition of atoms on this face in the following step. 26 As such, some of the nanocubes were elongated along one direction, generating nanobars with an aspect ratio slightly greater than one.

In a control experiment, we conducted the same synthesis without separating growth from nucleation by holding the reaction solution in a vial at 95 °C for 4 h. As shown in Figure 1c, the product contained a mixture of cubes, truncated bipyramids, decahedra, and rods at distributions of 64, 23, 9, and 4%, respectively, together with polydispersed sizes. The diversity in both shape and size could be attributed to the multiple nucleation events involved in the synthesis, during which different types of seeds were generated, followed by growth for different durations of time. It should be pointed out that there are well-developed protocols for the preparation of Pd nanocubes, and they typically involve the quick reduction of PdCl<sub>4</sub><sup>2-</sup> at an elevated temperature. The slow reduction kinetics of PdBr<sub>4</sub><sup>2-</sup> and a high concentration of KBr make this system unsuitable for the generation of single-crystal seeds using the conventional method. However, by optimizing the experimental conditions for nucleation and growth, and more importantly, separating them, uniform Pd nanocubes, as those shown in Figure 1b, could be readily obtained. Moreover, the Pd nanocubes reported here also showed improvement in quality when compared with those prepared following the conventional protocol (Figure S2).<sup>27</sup> As shown in Figure S3, despite the slight difference in size, greater focus on both the size and aspect ratio were observed for the Pd nanocubes synthesized by decoupling growth from nucleation relative to those prepared using the conventional method. The improvement in quality could be attributed to the elimination of multiple nucleation events in the synthesis and thus involvement of the same duration of growth for attaining a uniform size. Additionally, due to the involvement of a relatively low temperature for the growth step, localized oxidative etching was largely mitigated for the formation of more nanocrystals with a cubic shape. Taken together, by decoupling growth from nucleation, the as-obtained Pd nanocubes exhibited high uniformity in both size and shape.

Another control experiment was also conducted by following the standard protocol, except that a batch reactor was used to control the nucleation step, during which the reaction solution was heated in a 20 mL glass vial at 95 °C for 30 s and then cooled down in an ice bath. The Pd nanocrystals obtained after 48 h of growth at room temperature also exhibited various shapes and polydispersed sizes (Figure S4). Due to the involvement of a bulk amount of solution and a relatively short period of time, the spatial inhomogeneity in temperature, together with slow initiation and quenching of the reduction,

contributed to the formation of various types of seeds and thus polydispersed nanocrystals. This result clearly suggested the necessity of using a flow reactor to control the subtle nucleation step owing to its enhancement in heat transfer management. Besides, it is noteworthy that the flow reactor can also be easily and conveniently adapted for the scale-up production by running the synthesis continuously, offering a promising approach to the mass production of nanocrystals with high quality.

To validate that growth was decoupled from nucleation during the synthesis, we monitored the evolution of the nanocrystals prepared using the standard protocol by sampling and analyzing the reaction solution at different time points. Figure 2 shows TEM images of the corresponding products.

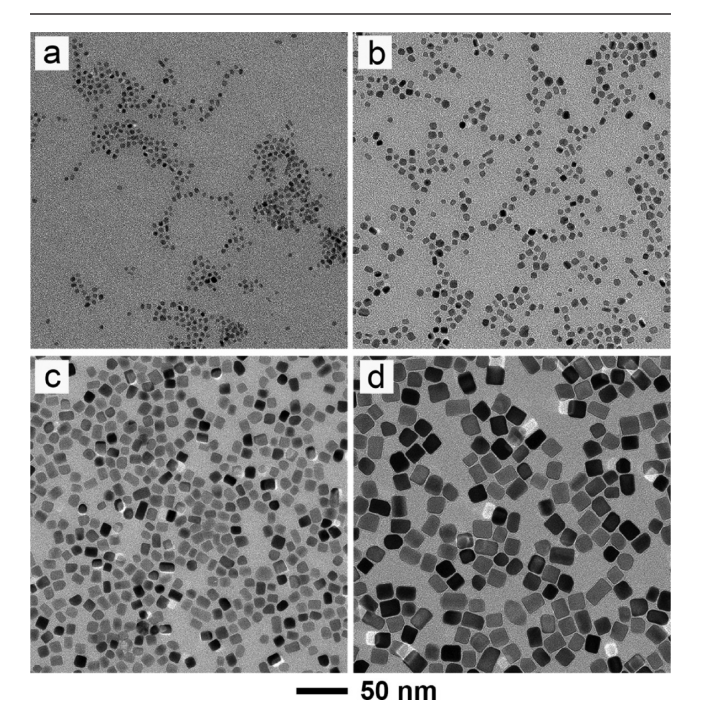


**Figure 2.** TEM images of the samples obtained using the standard protocol after (a) nucleation at 95  $^{\circ}$ C for 30 s and (b–d) nucleation at 95  $^{\circ}$ C for 30 s, followed by growth at room temperature for (b) 2, (c) 8, and (d) 24 h, respectively. The scale bar at the bottom applies to all panels.

After nucleation at 95 °C for 30 s, we obtained seeds featuring a nearly spherical shape, together with an average diameter of 2.9 nm. After growth at room temperature for 2 h, the seeds evolved into cuboctahedral nanocrystals with a size approaching 4.7 nm. When the growth time was extended to 8 h, almost all the nanocrystals evolved into nanocubes with slight truncation at the corners, while the average edge length increased to 9.5 nm. As the growth was continued for another 16 h, the edge length increased to 14.3 nm. Significantly, no second population of particles (typically, smaller in size than the main product) was observed during the entire growth process, excluding the possible involvement of additional nucleation events in the solution and attesting to the dominance of surface reduction during the growth process.

To verify that no additional homogeneous nucleation could take place in the solution phase during the growth stage, we analyzed the reduction kinetics using UV—vis spectroscopy. Two sets of measurements were conducted in parallel, with one sample prepared by following the standard protocol while

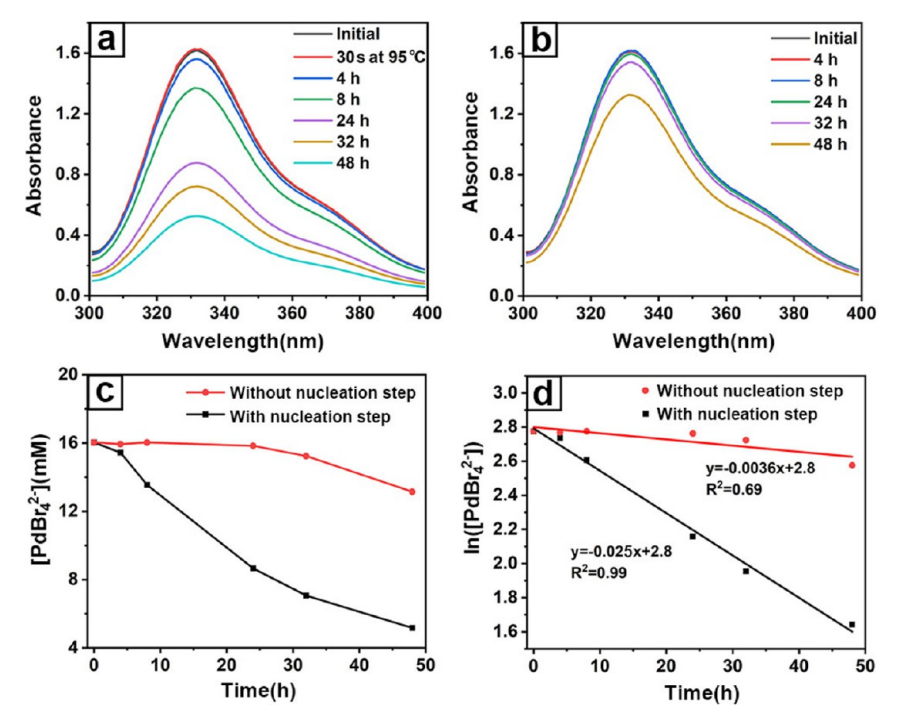


Figure 3. Quantitative analysis of the reduction kinetics involved in the synthesis. (a) UV–vis spectra of  $PdBr_4^{2-}$  remaining in the reaction solution after nucleation at 95 °C for 30 s and then growth at room temperature for different periods of time. (b) Time-dependent UV–vis spectra of the reaction solution stored at room temperature for different periods of time, without involving the prior nucleation step. (c) Plots of the concentrations of  $PdBr_4^{2-}$  remaining in the reaction solution over time, which were derived from the absorbance peak of  $PdBr_4^{2-}$  at 332 nm. (d) Plots showing the variation of  $ln[PdBr_4^{2-}]$  as a function of reaction time, suggesting a pseudo-first-order kinetics for the synthesis involving the nucleation step.

the other was directly kept at room temperature without undergoing the nucleation step at 95 °C (Figure 3a,b). At each time point, aliquots were sampled from the reaction solutions, followed by the immediate quenching of the reduction. We then recorded UV-vis spectra to derive the concentration of Pd(II) ions remaining in the solution by comparing the absorbance at 332 nm with the calibration curve in Figure S1. As shown in Figure 3c, for the synthesis involving the nucleation step, the concentration of the remaining PdBr<sub>4</sub><sup>2-</sup> gradually decreased over time, indicating the continuous growth of the preformed seeds in the solution. In contrast, without including the nucleation step, PdBr<sub>4</sub><sup>2-</sup> in the solution was barely reduced at room temperature over a period of 24 h and no significant change in the concentration was observed either until 32 h later. The sluggish reduction kinetics suggested the low possibility of additional homogeneous nucleation in the growth solution.

Typically, the reduction of a metal precursor by a reductant involves collision and electron transfer between them, and thus, the reaction is supposed to follow the second-order rate law with regard to the concentrations of both the precursor and reductant. <sup>29</sup> In the present study, however, the amount of the reductant, AA, was used in large excess relative to the precursor. As such, the concentration of AA can be regarded as a constant during the synthesis, and thus, the reduction kinetics can be simplified to the pseudo-first-order rate law, with a linear dependence between  $ln[PdBr_4^{\ 2-}]$  and reaction time. Figure 3d shows a plot of the value of  $ln[PdBr_4^{\ 2-}]$  as a function of time, confirming the pseudo-first-order kinetics for the synthesis involving the nucleation step. In comparison, the data for the synthesis involving no nucleation step did not fit the pseudo-first-order kinetics well, with a small  $R^2$  of 0.69.

The poor fitting can be ascribed to the slow reduction kinetics and the difficulty in initiating the nucleation.

The observed difference in the reduction kinetics of these two samples clearly demonstrated the low probability of homogeneous nucleation during the growth stage in the standard synthesis. In the absence of preformed seeds from the nucleation at an elevated temperature, the reduction of PdBr<sub>4</sub><sup>2-</sup> by AA at room temperature could only take place in the solution phase. As shown in Figure 3b,c, the solution reduction proceeded at an extremely slow rate, inherently restraining the occurrence of homogeneous nucleation. On the other hand, in the presence of preformed seeds, the reduction of PdBr<sub>4</sub><sup>2-</sup> favored the surface reduction pathway due to its much lower activation energy barrier. 14 As such, the reduction of the precursor would be able to occur but is mainly confined to the surface of the seeds, while homogeneous nucleation was essentially suppressed. With the continuous consumption of the reactant, the concentration of PdBr<sub>4</sub><sup>2-</sup> quickly decreased, as shown in Figure 3a,c, further diminishing the probability of additional homogeneous nucleation in the solution phase. Moreover, as demonstrated in a recent study, halide ions could control the growth pattern of Pd nanocrystals by preventing the precursor from hydrolysis and slowing down the reduction kinetics.<sup>25</sup> Specifically, in the presence of cubic seeds, when the molar ratio of KBr to the precursor was set to 30 (the same as what was used in the present study), surface reduction prevailed over solution reduction by a ratio of 99 to 1. These results were consistent with the TEM images shown in Figure 2, where no second population of small particles were observed. Collectively, it can be concluded that the growth process was free of additional, unwanted nucleation events owing to the dominance of surface reduction.

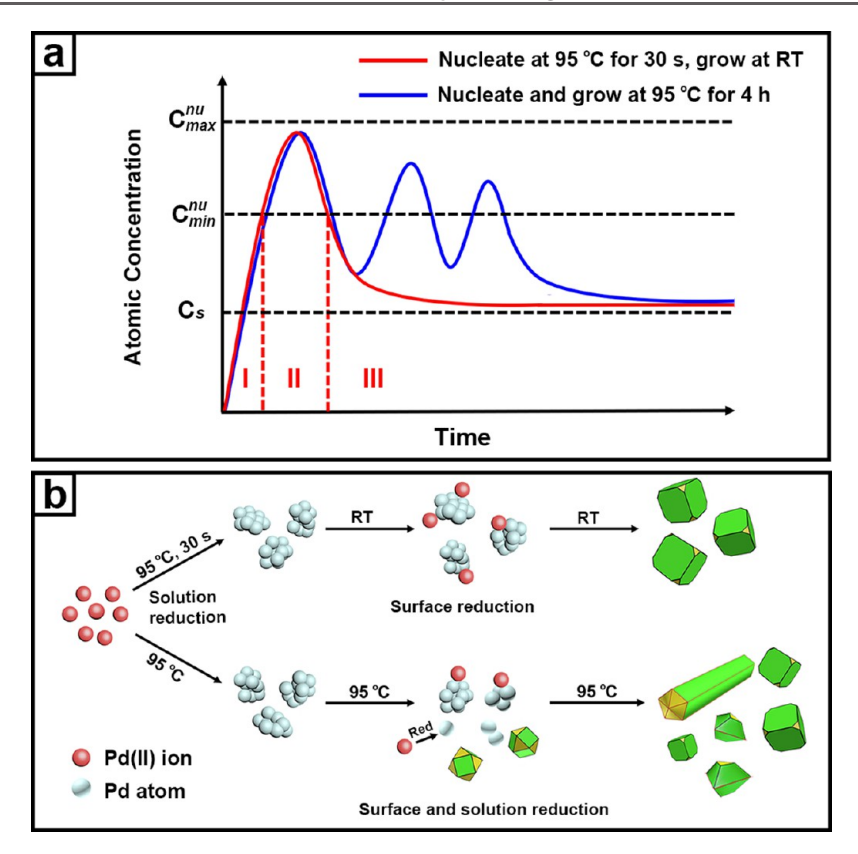


Figure 4. (a) Comparison of the nucleation and growth processes involved in the two syntheses shown in Figure 1b,c, respectively. In the framework of LaMer model, stages I, II, and III correspond to the generation of atoms, nucleation, and growth, respectively. (b) Schematic illustration of the reduction pathways involved in the two syntheses. After heating at 95 °C for 30 s, small nuclei were formed, which subsequently grew into uniform nanocubes through surface reduction at room temperature. In contrast, when the synthesis was conducted at 95 °C for 4 h, both surface and solution reduction were allowed, leading to the continuous generation of seeds throughout the synthesis and thus the formation of nanocrystals with broad sizes and diverse shapes.

On the basis of the above results, we can explain the difference between the Pd nanocrystals prepared with and without separating growth from nucleation (Figure 1b,c) using the LaMer model (Figure 4a) and the reduction pathways involved in the synthesis (Figure 4b). The mechanism underlying the formation of uniform colloidal nanocrystals has been extensively studied and can be described using the LaMer model.<sup>6,7</sup> In the synthesis of metal nanocrystals, as the precursor is continuously reduced, the concentration of metal atoms in the solution increases with time (stage I). Once the atomic concentration exceeds the threshold of nucleation  $(C_{\min}^{\text{nu}})$ , the aggregation or assembly of metal atoms leads to the formation of nuclei (stage II). Meanwhile, the rapid consumption of atoms results in the quick decrease in the concentration, and homogeneous nucleation will be terminated once the atomic concentration drops below the minimum level of supersaturation needed for nucleation. The nuclei then evolve into seeds, followed by growth to larger nanocrystals (stage III). In this context, to obtain nanocrystals with a narrow distribution in size, the peak corresponding to nucleation is supposed to be as sharp as possible for the initiation of a single burst of nucleation only. In other words, a broad peak would lead to a longer time for nucleation and thus, the nuclei formed at different time points would go through different growth histories, generating nanocrystals with a broad distribution in size. Different from the conventional synthesis conducted in a batch reactor, when a fluidic device is used to control the nucleation step, the

precursor can be quickly reduced at 95 °C in the solution so that homogeneous nucleation can be initiated and confined to a very short, single burst of 30 s. Afterward, by taking advantage of the well-regulated slow reduction kinetics, the seeds can grow to larger nanocrystals at room temperature through the surface reduction of the precursor, due to its lower activation energy barrier relative to that for solution reduction. During growth, no additional nucleation events will be able to occur in the solution phase, resulting in the formation of highly uniform nanocrystals.

In contrast, multiple nucleation events took place when the synthesis was conducted at 95 °C for 4 h without separating growth from nucleation. After a burst of nucleation, the concentration of atoms would drop quickly but increase again thereafter due to the continuous supply of Pd atoms at such a high temperature, leading to new rounds of nucleation. In this case, the atomic concentration tended to fluctuate above and below the threshold of nucleation several times, resulting in a long period of nucleation and thus the polydispersity in terms of size. From the viewpoint of reduction pathway, both surface and solution reduction were involved in the growth stage. At 95 °C, a temperature high enough for solution reduction to overcome its activation energy barrier, the reduction of the precursor proceeded not only on the surface of the preformed seeds for growth but also in the solution phase to initiate homogeneous nucleation and generate new seeds continually. Moreover, the reduction rate would decrease with the continuous consumption of the precursor. It has been

demonstrated that the seeds formed in the synthesis of Pd nanocrystals would switch from a single crystal to multitwinned and then stacking-fault-lined structures as the reduction rate decreased. As a result, the final products contained truncated bipyramids, decahedra, and pentatwinned nanorods growing from the seeds with twin defects. Taken together, it is the continuous formation of seeds during the synthesis that results in the variation in the seed type, as well as the diversity in shape and broad distribution in the size of the final products.

In addition to improving the product quality, setting apart growth from nucleation also offers a means to differentiate the seeds formed in the initial stages of the synthesis and resolve the details of the vital but subtle nucleation process. To investigate how the length of the time for nucleation affects the formation of seeds and the resultant nanocrystals, a set of experiments were conducted with different durations of nucleation. It is worth pointing out that the retention time of the reaction solution (i.e., the duration of nucleation) is determined by both the flow rate and the length of the tube subjected to heating. At a fixed length for the tubular reactor, increasing the flow rate may cause additional issues because of the parabolic distribution of velocities associated with the flow. 16,30 In principle, a high flow rate will lead to greater variations among the velocities at different radial positions of the flow and thus different lengths of the retention time for the reaction solution. Therefore, it would be difficult to precisely control the duration for nucleation, resulting in size polydispersity for the obtained nanocrystals. Although a moderate flow rate of 2 mL/min used in the standard synthesis, and an even higher rate of 3 mL/min, did not induce a broad size distribution for the resultant nanocubes, further increasing the flow rate may eventually cause size distribution broadening. Therefore, instead of varying the flow rate, we changed the duration of nucleation by adjusting the length of the PTFE tube subjected to heating at 95 °C. Figure 5a-d shows TEM images of the corresponding Pd nanocrystals obtained when the durations of nucleation were set to 10, 20, 60, and 120 s, respectively. Interestingly, when the nucleation time was as short as 10 s, the final product contained both large nanocubes and truncated bipyramids, suggesting the formation of both single-crystal and single-twinned seeds in the nucleation step. The formation of seeds with a single twin plane could be attributed to the relatively slow reduction rate in the very first few seconds of nucleation before the temperature of the reaction solution reached 95 °C. In comparison, as the nucleation time was prolonged to 20, 30, 60, and 120 s, the twinned structure disappeared, while only nanocubes were obtained as the final products. This could be ascribed to the oxidative etching involved in the synthesis. In the presence of Br ions and O2 dissolved in the reaction solution, which could form an etchant, the twinned seeds could be selectively removed while the single-crystal seeds were retained.31,32 When the nucleation time was only 10 s, the twinned seeds could not be fully removed by oxidative etching, accounting for the formation of truncated bipyramids. As the nucleation time was prolonged, all the twinned seeds formed in the early nucleation stages could be completely etched away, leaving behind single-crystal seeds for their growth into nanocubes. To verify the proposed mechanism, the control experiment was conducted by following the standard protocol except that the reaction solution was bubbled with argon before the nucleation step to remove the dissolved O2. As

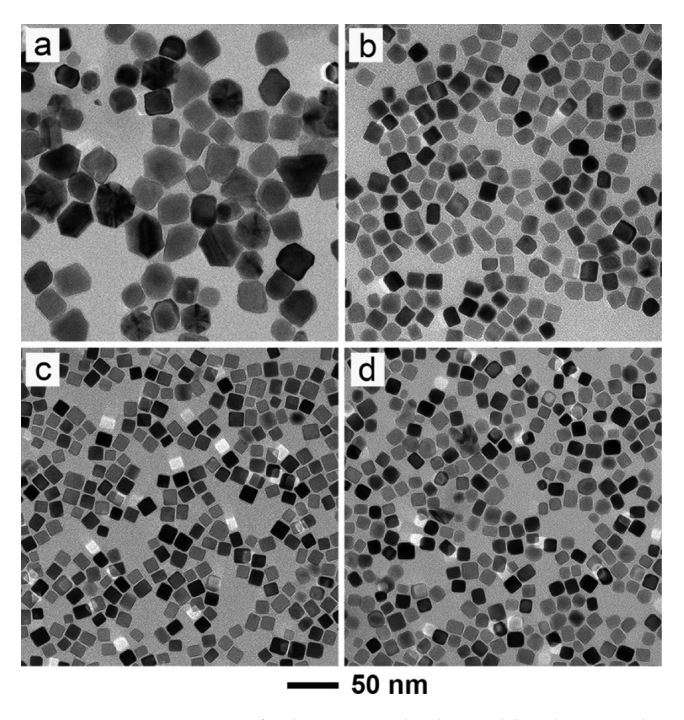


**Figure 5.** TEM images of Pd nanocrystals obtained by changing the nucleation time at 95 °C from 30 s to (a) 10, (b) 20, (c) 60, and (d) 120 s, respectively. As the duration of nucleation was increased, products bearing a singly-twinned structure disappeared while the Pd nanocubes became smaller and less uniform in terms of size.

expected, twinned structures appeared in the final product (Figure S5) due to the lack of oxidative etching during the nucleation step.

Moreover, as shown in Figure 5b-d, although the products were dominated by nanocubes when the nucleation time was longer than 10 s, the sizes of the nanocrystals became smaller and less uniform with the increase in nucleation time. When the nucleation time was set to 20, 60, and 120 s, the average edge length of the nanocubes decreased from 19.0  $\pm$  1.5 to  $12.9 \pm 2.2$  nm and then  $12.1 \pm 2.6$  nm. This could be rationalized by the increased number of seeds produced as the duration of nucleation was prolonged. With more seeds formed, less Pd atoms would be allocated to each seed for growth because the amount of the precursor fed into the reaction was fixed, generating smaller nanocrystals. Furthermore, the seeds formed in the earlier stage of nucleation would grow into larger nanocrystals compared with those formed later owing to their longer growth times. As a result, the products would become less uniform in terms of size, in agreement with the trend in that the standard deviation of the size increased with the nucleation time. Taken together, the duration of nucleation should be optimized for the formation of single-crystal seeds, while confining the nucleation to a short burst to ensure a narrow size distribution.

Besides duration, the influence of the temperature on the nucleation was also studied. Because the synthesis was conducted in an aqueous phase, we only lowered the temperature for triggering nucleation from 95 to 80 and 65 °C. In contrast to the uniform nanocubes produced using the standard protocol, nanocrystals with large sizes and poorly defined shapes, such as concave cubes and decahedra covered by rough surfaces, were obtained as the temperature for nucleation was reduced to 80 °C (Figure 6a). Owing to the decreased reduction rate at a lower temperature, both single-

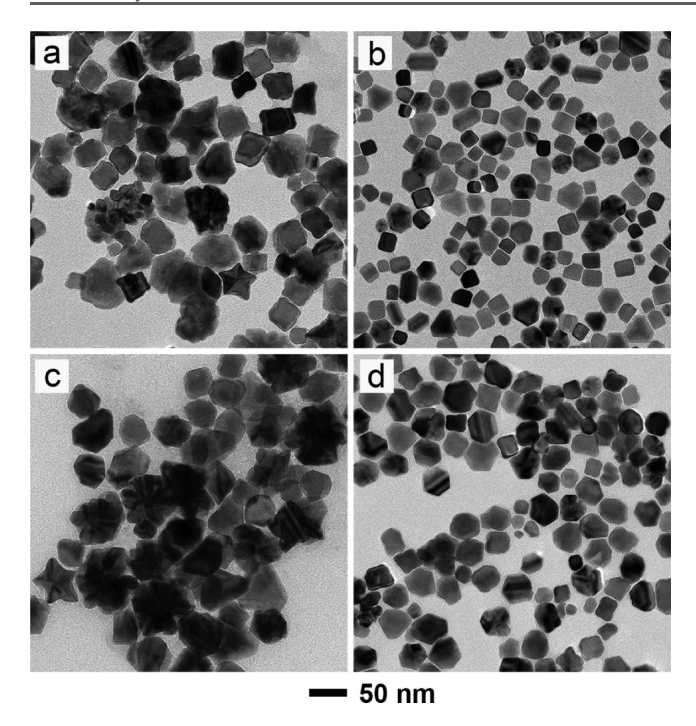


**Figure 6.** TEM images of Pd nanocrystals obtained by changing the temperature and duration for nucleation from 95 °C/30 s to (a) 80 °C/30 s, (b) 80 °C/60 s, (c) 65 °C/60 s, and (d) 65 °C/120 s, respectively. As the temperature dropped, nanocrystals featuring twinned structures and irregular shapes could be easily observed.

crystal and multitwinned seeds were generated in the nucleation step and at a smaller total number than the case of 95 °C. Therefore, more precursors would be available to each seed during subsequent growth, producing nanocrystals with larger sizes. The irregular shapes could be attributed to the limited surface diffusion at a lower temperature and therefore symmetry reduction. When the nucleation at 80 °C was prolonged to 60 s (Figure 6b), the product became smaller while the shape could be clearly resolved as a mix of truncated cubes and nanocrystals with twinned structures, including penta-twinned nanorods and truncated bipyramids. These observations suggest that the type of seeds formed in the nucleation stage changed from the single crystal to both singlecrystal and twinned structures when the temperature for nucleation decreased to 80 °C. We also conducted experiments by allowing the nucleation to proceed at 65 °C for 60 and 120 s (Figure 6c,d), and the results trend in the same pattern as those obtained at 80 °C. Moreover, due to the further deceleration of reduction at 65 °C, more twinned nanocrystals, as well as a broader size distribution, were observed in the final products. Collectively, these results were in agreement with our previous study in that the type of seeds formed in the synthesis tended to shift from single crystal to multitwinned as the reduction rate decreased.<sup>29</sup> It should be noted that in the present work, the oil bath was held at a temperature slightly lower than the boiling point of the solvent to ensure the fast reduction kinetics for the nucleation process, and thus a burst of nucleation as well as the generation of single-crystal seeds to form cubes. If the temperature is further increased, the pressure built up in the tubular reactor would make it challenging to handle the reaction system. Nevertheless, when extending this strategy to the synthesis of other metal nanocrystals taking different shapes, the close correlation

between the initial reduction rate of the synthesis and the type of seeds generated after nucleation should be taken into consideration.<sup>29</sup> A higher temperature and thus a faster reduction rate for the nucleation step favors the generation of single-crystal seeds, while a lower temperature could trigger the formation of seeds with multitwinned or stacking fault-lined structures owing to the slower reduction kinetics. Therefore, the temperature of the oil bath should be judiciously controlled to obtain seeds with a specific type of internal structure for the target product. By setting apart nucleation and growth, we can explicitly study the mechanistic details about the nucleation step for the deterministic production of seeds with a specific structure due to the exclusion of multiple nucleation events under the complicated and dynamic conditions of the synthesis.

We also extended the synthetic strategy to the preparation of Pt nanocubes. To date, much effort has been devoted to controlling the synthesis of Pt nanocrystals due to their outstanding performance in a number of electrocatalytic reactions and industrial processes.<sup>2,33–35</sup> In particular, the uniformity of Pt nanocrystals in terms of shape and size is critical to their catalytic performance. If the size is polydispersed, sintering would be induced by Ostwald ripening, resulting in the loss of the specific surface area and thus catalytic activity. 36,37 By decoupling growth from nucleation in a polyol synthesis, we successfully achieved the production of sub-5 nm Pt nanocubes in high uniformity. The synthetic procedure is similar to that for Pd, except that a Pt(IV) precursor was reduced by EG in the presence of KBr and PVP. At a high temperature of 185 °C, the homogeneous nucleation was enabled in a tubular flow reactor for 60 s, generating seeds with an average size of 3.1 nm (Figure S6). After quenching the reduction, the collected solution was then kept at 110 °C for 48 h, allowing the just-formed seeds to grow into nanocubes with a uniform size of  $3.9 \pm 0.5$  nm due to the capping effect of Br ions toward Pt{100} (Figures 7a and S7a). After a close examination of over 680 particles, more than 95% of the nanocrystals are well-defined nanocubes or slightly truncated cubes, demonstrating the high purity of the products. In contrast, when the polyol synthesis was conducted in a vial at 185 °C for 8 h, a large quantity of particles with rounded or irregular shapes were observed in the products, in addition to cubes at a purity of 61%, suggesting the occurrence of multiple nucleation events in the synthesis (Figure 7b). With an average size of  $4.1 \pm 1.0$  nm, the polydispersity of the products was confirmed by the wider peak observed in the size distribution, as well as a difference of around 7 nm between the maximum and minimum sizes (Figure S7b), which could cause sintering and be detrimental to their use in catalytic applications. Besides, significant aggregation was also observed in this sample, likely due to the formation of a large number of seeds in the multiple nucleation events and thus an insufficient amount of PVP to stabilize all the particles.

Different from the case of Pd, the growth of Pt seeds was performed at a judiciously selected temperature of 110 °C instead of room temperature to achieve both a slow reduction rate and sufficient atom diffusion because of the higher bonding energy of Pt relative to that of Pd ( $E_{\rm Pd-Pd}=136~{\rm kJ/mol}$ ). We also varied the temperature for growth to investigate its impact on the resultant Pt nanocrystals while keeping all other experimental parameters the same. When the temperature for growth was lowered to  $100~{\rm ^{\circ}C}$ , only a small fraction of the Pt nanocrystals was able to

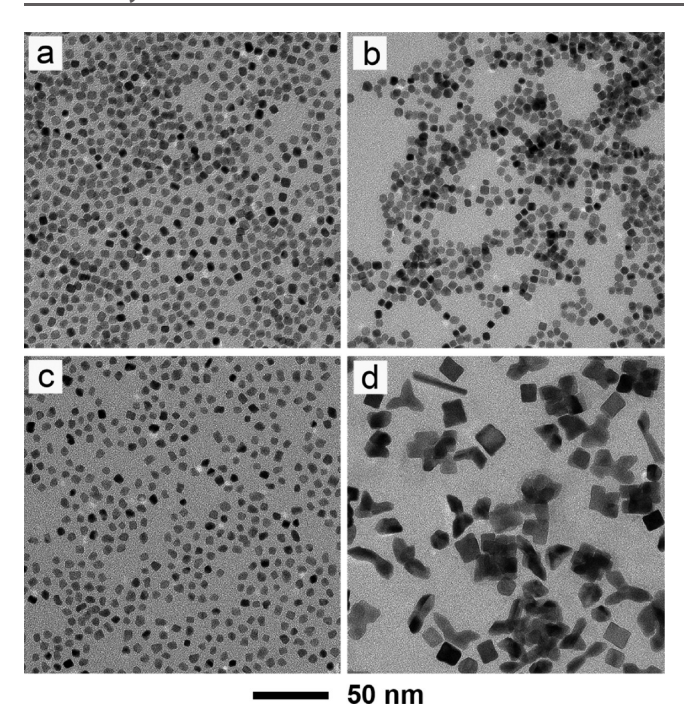


**Figure 7.** (a) TEM image of Pt nanocubes obtained by conducting the nucleation at 185 °C for 60 s, followed by growth at 110 °C for 48 h. (b) TEM image of Pt nanocrystals prepared by conducting the synthesis in a vial at 185 °C for 8 h. (c,d) TEM images of Pt nanocrystals obtained by allowing the nucleation to proceed at 185 °C for 60 s, followed by growth at (c) 100 and (d) 140 °C for 48 h, respectively.

develop into nanocubes because of the noticeably slower reduction rate (Figure 7c). In comparison, at a higher temperature of 140 °C, the reduction rate was greatly accelerated to overwhelm atom diffusion, resulting in the growth of the seeds into concave cubes and octapods (Figure 7d). Besides, it is evident that additional nucleation events also took place during the growth stage, giving rise to particles with irregular shapes and polydispersed size distribution. In view of this, a moderate temperature of 110 °C is critical to enabling the reduction of the precursor on the surface of Pt seeds for their growth into cubes while suppressing homogeneous nucleation in the solution phase and thus the formation of undesired seeds.

Until now, only limited success has been achieved in the synthesis of sub-5 nm Pt nanocubes, during which the high pressure of CO is typically involved. 38 The high toxicity and flammability of CO might lead to concerns in safety issues and potential pollution to the environment. In the present study, by separating growth from nucleation, the single burst of nucleation ensured the generation of a large number of seeds in high purity, while the slow growth rate contributed to the achievement of a small particle size. Through the judicious management of nucleation and growth in the polyol synthesis, sub-5 nm Pt nanocubes could be readily obtained without the involvement of CO. The tight control over the shape and size uniformity of the products might help mitigate sintering and thereby improve the stability of Pt nanocrystals in catalytic applications. Furthermore, taking the advantage of a flow reactor in scaling up the synthesis continuously, it is feasible to achieve mass production of sub-5 nm Pt nanocubes without compromising product quality, pushing the Pt nanocrystals closer to practical use.

#### CONCLUSIONS

In summary, we have integrated the use of a flow reactor with the manipulation of the reduction pathway of a precursor to decouple growth from nucleation for the achievement of a better control over colloidal metal nanocrystals. With Pd as an example, we obtained uniform Pd nanocubes by thermally triggering the nucleation at 95 °C for a very short period of time in the reaction solution flowing in a tubular reactor, followed by the growth of the just-formed seeds at room temperature through surface reduction. A quantitative analysis of the reduction kinetics, together with the characterization of the products obtained at different stages, confirmed that no additional, undesired nucleation event took place during the growth process, accounting for the high purity and uniformity of the products. Unlike the conventional synthesis, in which multiple nucleation events tend to occur even during the growth stage, decoupling growth from nucleation can well preserve the seeds formed in the initial stage of the synthesis, while directly enhancing the quality of the resultant nanocrystals. It was revealed that both the duration and temperature for nucleation had a profound impact on the type and quality of the seeds and thus the resultant nanocrystals, offering insightful information on the significant but subtle nucleation process. With such insights into the mechanistic details of nucleation, one can achieve a tighter control over the synthesis for the deterministic production of seeds with specific internal structures and thus nanocrystals with the desired shapes and sizes. This method was further extended to the synthesis of highly uniform, sub-5 nm Pt nanocubes, suggesting the potential of this approach for the preparation of other colloidal metal nanocrystals. We believe this work not only deepens our understanding of the mechanistic details involved in nucleation and growth but also improves our synthetic capability to produce nanocrystals with good uniformity in terms of sizes and shapes. The high uniformity and purity of the as-obtained nanocrystals are expected to enhance their performance in various applications.

### ASSOCIATED CONTENT

# **S** Supporting Information

The Supporting Information is available free of charge at https://pubs.acs.org/doi/10.1021/acs.chemmater.1c00923.

UV-vis spectra and calibration curve of a set of PdBr<sub>4</sub><sup>2-</sup> solutions with different concentrations, TEM images of various Pd and Pt nanocrystals prepared under different reaction conditions, and plots showing the size and aspect ratio distribution of the Pd and Pt nanocrystals (PDF)

# AUTHOR INFORMATION

#### **Corresponding Author**

Younan Xia — School of Chemistry and Biochemistry and School of Chemical and Biomolecular Engineering, Georgia Institute of Technology, Atlanta, Georgia 30332, United States; The Wallace H. Coulter Department of Biomedical Engineering, Georgia Institute of Technology and Emory University, Atlanta, Georgia 30332, United States; orcid.org/0000-0003-2431-7048; Email: younan.xia@bme.gatech.edu

# **Authors**

Ruhui Chen — School of Chemistry and Biochemistry, Georgia Institute of Technology, Atlanta, Georgia 30332, United States; © orcid.org/0000-0003-4163-6964

Zhiheng Lyu — School of Chemistry and Biochemistry, Georgia Institute of Technology, Atlanta, Georgia 30332, United States; © orcid.org/0000-0002-1343-4057

Yifeng Shi — School of Chemical and Biomolecular Engineering, Georgia Institute of Technology, Atlanta, Georgia 30332, United States

Complete contact information is available at: https://pubs.acs.org/10.1021/acs.chemmater.1c00923

#### **Notes**

The authors declare no competing financial interest.

## ACKNOWLEDGMENTS

This work was supported in part by a research grant from the NSF (CHE-1804970) and start-up funds from the Georgia Institute of Technology. TEM imaging was performed at the Georgia Tech Institute for Electronics and Nanotechnology, a member of the National Nanotechnology Coordinated Infrastructure (NNCI), which is supported by the National Science Foundation (ECCS-2025462).

# REFERENCES

- (1) Tao, A. R.; Habas, S.; Yang, P. Shape Control of Colloidal Metal Nanocrystals. *Small* **2008**, *4*, 310–325.
- (2) Peng, Z.; Yang, H. Designer Platinum Nanoparticles: Control of Shape, Composition in Alloy, Nanostructure and Electrocatalytic Property. *Nano Today* **2009**, *4*, 143–164.
- (3) Liu, H.-l.; Nosheen, F.; Wang, X. Noble Metal Alloy Complex Nanostructures: Controllable Synthesis and Their Electrochemical Property. *Chem. Soc. Rev.* **2015**, *44*, 3056–3078.
- (4) Zhang, H.; Jin, M.; Xiong, Y.; Lim, B.; Xia, Y. Shape-Controlled Synthesis of Pd Nanocrystals and Their Catalytic Applications. *Acc. Chem. Res.* **2013**, *46*, 1783–1794.
- (5) Chen, Q.; Jia, Y.; Xie, S.; Xie, Z. Well-Faceted Noble-Metal Nanocrystals with Nonconvex Polyhedral Shapes. *Chem. Soc. Rev.* **2016**, *45*, 3207–3220.
- (6) LaMer, V. K.; Dinegar, R. H. Theory, Production and Mechanism of Formation of Monodispersed Hydrosols. *J. Am. Chem. Soc.* **1950**, 72, 4847–4854.
- (7) Xia, Y.; Xiong, Y.; Lim, B.; Skrabalak, S. E. Shape-Controlled Synthesis of Metal Nanocrystals: Simple Chemistry Meets Complex Physics? *Angew. Chem., Int. Ed.* **2009**, *48*, 60–103.
- (8) Xia, Y.; Gilroy, K. D.; Peng, H.-C.; Xia, X. Seed-Mediated Growth of Colloidal Metal Nanocrystals. *Angew. Chem., Int. Ed.* **2017**, 56, 60–95.
- (9) Janssen, A.; Shi, Y.; Xia, Y. Separating Growth from Nucleation for Facile Control over the Size and Shape of Palladium Nanocrystals. *Chem.*—Eur. J. 2020, 26, 13890–13895.
- (10) Thanh, N. T. K.; Maclean, N.; Mahiddine, S. Mechanisms of Nucleation and Growth of Nanoparticles in Solution. *Chem. Rev.* **2014**, *114*, 7610–7630.
- (11) Watzky, M. A.; Finke, R. G. Transition Metal Nanocluster Formation Kinetic and Mechanistic Studies. A New Mechanism When Hydrogen Is the Reductant: Slow, Continuous Nucleation and Fast Autocatalytic Surface Growth. *J. Am. Chem. Soc.* **1997**, *119*, 10382–10400.
- (12) Watzky, M. A.; Finney, E. E.; Finke, R. G. Transition-Metal Nanocluster Size vs Formation Time and the Catalytically Effective Nucleus Number: A Mechanism-Based Treatment. *J. Am. Chem. Soc.* **2008**, *130*, 11959–11969.
- (13) Yang, T.-H.; Zhou, S.; Gilroy, K. D.; Figueroa-Cosme, L.; Lee, Y.-H.; Wu, J.-M.; Xia, Y. Autocatalytic Surface Reduction and its Role

- in Controlling Seed-Mediated Growth of Colloidal Metal Nanocrystals. Proc. Natl. Acad. Sci. U.S.A. 2017, 114, 13619-13624.
- (14) Yang, T.-H.; Peng, H.-C.; Zhou, S.; Lee, C.-T.; Bao, S.; Lee, Y.-H.; Wu, J.-M.; Xia, Y. Toward a Quantitative Understanding of the Reduction Pathways of a Salt Precursor in the Synthesis of Metal Nanocrystals. *Nano Lett.* **2017**, *17*, 334–340.
- (15) Niu, G.; Ruditskiy, A.; Vara, M.; Xia, Y. Toward Continuous and Scalable Production of Colloidal Nanocrystals by Switching from Batch to Droplet Reactors. *Chem. Soc. Rev.* **2015**, *44*, 5806–5820.
- (16) Song, H.; Tice, J. D.; Ismagilov, R. F. A Microfluidic System for Controlling Reaction Networks in Time. *Angew. Chem.* **2003**, *42*, 768–772.
- (17) Marre, S.; Jensen, K. F. Synthesis of Micro and Nanostructures in Microfluidic Systems. *Chem. Soc. Rev.* **2010**, *39*, 1183–1202.
- (18) Yen, B. K. H.; Stott, N. E.; Jensen, K. F.; Bawendi, M. G. A Continuous-Flow Microcapillary Reactor for the Preparation of a Size Series of CdSe Nanocrystals. *Adv. Mater.* **2003**, *15*, 1858–1862.
- (19) Jahn, A.; Reiner, J. E.; Vreeland, W. N.; DeVoe, D. L.; Locascio, L. E.; Gaitan, M. Preparation of Nanoparticles by Continuous-Flow Microfluidics. *J. Nanopart. Res.* **2008**, *10*, 925–934.
- (20) Abou-Hassan, A.; Sandre, O.; Neveu, S.; Cabuil, V. Synthesis of Goethite by Separation of the Nucleation and Growth Processes of Ferrihydrite Nanoparticles Using Microfluidics. *Angew. Chem., Int. Ed.* **2009**, *48*, 2342–2345.
- (21) Pan, J.; El-Ballouli, A. a. O.; Rollny, L.; Voznyy, O.; Burlakov, V. M.; Goriely, A.; Sargent, E. H.; Bakr, O. M. Automated Synthesis of Photovoltaic-Quality Colloidal Quantum Dots Using Separate Nucleation and Growth Stages. *ACS Nano* **2013**, *7*, 10158–10166.
- (22) Kim, K.-J.; Oleksak, R. P.; Hostetler, E. B.; Peterson, D. A.; Chandran, P.; Schut, D. M.; Paul, B. K.; Herman, G. S.; Chang, C.-H. Continuous Microwave-Assisted Gas-Liquid Segmented Flow Reactor for Controlled Nucleation and Growth of Nanocrystals. *Cryst. Growth Des.* 2014, 14, 5349–5355.
- (23) Albuquerque, G. H.; Squire, K.; Wang, A. X.; Herman, G. S. Continuous Synthesis of Monodisperse Ag Nanocubes. *Cryst. Growth Des.* **2018**, *18*, 119–125.
- (24) Xie, M.; Zhou, S.; Zhu, J.; Lyu, Z.; Chen, R.; Xia, Y. A Quantitative Analysis of the Reduction Kinetics Involved in the Synthesis of Au@Pd Concave Nanocubes. *Chem.—Eur. J.* **2019**, 25, 16397–16404.
- (25) Yang, T. H.; Zhou, S.; Zhao, M.; Xia, Y. Quantitative Analysis of the Multiple Roles Played by Halide Ions in Controlling the Growth Patterns of Palladium Nanocrystals. *ChemNanoMat* **2020**, *6*, 576–588.
- (26) Xiong, Y.; Cai, H.; Wiley, B. J.; Wang, J.; Kim, M. J.; Xia, Y. Synthesis and Mechanistic Study of Palladium Nanobars and Nanorods. *J. Am. Chem. Soc.* **2007**, *129*, 3665–3675.
- (27) Jin, M.; Liu, H.; Zhang, H.; Xie, Z.; Liu, J.; Xia, Y. Synthesis of Pd Nanocrystals Enclosed by {100} Facets and with Sizes < 10 nm for Application in CO Oxidation. *Nano Res.* **2011**, *4*, 83–91.
- (28) Niu, W.; Li, Z.-Y.; Shi, L.; Liu, X.; Li, H.; Han, S.; Chen, J.; Xu, G. Seed-Mediated Growth of Nearly Monodisperse Palladium Nanocubes with Controllable Sizes. *Cryst. Growth Des.* **2008**, *8*, 4440–4444.
- (29) Wang, Y.; Peng, H.-C.; Liu, J.; Huang, C. Z.; Xia, Y. Use of Reduction Rate as a Quantitative Knob for Controlling the Twin Structure and Shape of Palladium Nanocrystals. *Nano Lett.* **2015**, *15*, 1445–1450.
- (30) Winterton, J. D.; Myers, D. R.; Lippmann, J. M.; Pisano, A. P.; Doyle, F. M. A Novel Continuous Microfluidic Reactor Design for the Controlled Production of High-Quality Semiconductor Nanocrystals. *J. Nanopart. Res.* **2008**, *10*, 893–905.
- (31) Cobley, C. M.; Skrabalak, S. E.; Campbell, D. J.; Xia, Y. Shape-Controlled Synthesis of Silver Nanoparticles for Plasmonic and Sensing Applications. *Plasmonics* **2009**, *4*, 171–179.
- (32) Xiong, Y.; Chen, J.; Wiley, B.; Xia, Y.; Aloni, S.; Yin, Y. Understanding the Role of Oxidative Etching in the Polyol Synthesis of Pd Nanoparticles with Uniform Shape and Size. *J. Am. Chem. Soc.* **2005**, *127*, 7332–7333.

- (33) Shi, Y.; Lyu, Z.; Zhao, M.; Chen, R.; Nguyen, Q. N.; Xia, Y. Noble-Metal Nanocrystals with Controlled Shapes for Catalytic and Electrocatalytic Applications. *Chem. Rev.* **2021**, *121*, 649–735.
- (34) Sui, S.; Wang, X.; Zhou, X.; Su, Y.; Riffat, S.; Liu, C.-j. A Comprehensive Review of Pt Electrocatalysts for the Oxygen Reduction Reaction: Nanostructure, Activity, Mechanism and Carbon Support in PEM Fuel Cells. *J. Mater. Chem. A* **2017**, *5*, 1808–1825.
- (35) Zang, W.; Li, G.; Wang, L.; Zhang, X. Catalytic Hydrogenation by Noble-Metal Nanocrystals with Well-Defined Facets: a Review. *Catal. Sci. Technol.* **2015**, *5*, 2532–2553.
- (36) Hansen, T. W.; DeLaRiva, A. T.; Challa, S. R.; Datye, A. K. Sintering of Catalytic Nanoparticles: Particle Migration or Ostwald Ripening? *Acc. Chem. Res.* **2013**, *46*, 1720–1730.
- (37) Wettergren, K.; Schweinberger, F. F.; Deiana, D.; Ridge, C. J.; Crampton, A. S.; Rötzer, M. D.; Hansen, T. W.; Zhdanov, V. P.; Heiz, U.; Langhammer, C. High Sintering Resistance of Size-Selected Platinum Cluster Catalysts by Suppressed Ostwald Ripening. *Nano Lett.* 2014, 14, 5803–5809.
- (38) Wu, B.; Zheng, N.; Fu, G. Small Molecules Control the Formation of Pt Nanocrystals: a Key Role of Carbon Monoxide in the Synthesis of Pt Nanocubes. *Chem. Commun.* **2011**, *47*, 1039–1041.